

High-resolution genetic mapping of the mucosa-associated gut microbiome in hybrid mice provides novel insight on the impact of host genetics

Shauni Doms^{1,2}, Hanna Fokt^{1,2}, Malte Christoph Rühlemann^{3,4}, Cecilia J. Chung^{1,2}, Axel Künstner⁵, Saleh Ibrahim⁵, Andre Franke³, Leslie M. Turner^{7*†} and John F. Baines^{1,2*†}

¹ Max Planck Institute for Evolutionary Biology, Plön, Germany

² Section of Evolutionary Medicine, Institute for Experimental Medicine, Kiel University, Kiel, Germany

³ Institute for Clinical Molecular Biology (IKMB), Kiel University, Kiel Germany

⁴ Institute for Medical Microbiology and Hospital Epidemiology, Hannover Medical School, Hannover, Germany

⁵ Institute of Experimental Dermatology, University of Lübeck, Lübeck, Germany

⁶ Sharjah Institute of Medical Research, Sharjah, UAE

⁷ Milner Centre for Evolution, Department of Biology & Biochemistry, University of Bath, United Kingdom

* Correspondence: l.m.turner@bath.ac.uk; baines@evolbio.mpg.de

† These authors contributed equally to this work.

Further information and requests for resources and materials should be directed to and will be fulfilled by the lead contact, John F. Baines (baines@evolbio.mpg.de).

Abstract: Determining the forces that shape diversity in host-associated bacterial communities is critical to understanding the evolution and maintenance of meta-organisms. To gain novel insight on the genetics of gut microbial traits, we employed a powerful approach using inbred lines derived from the hybrid zone of two incipient house mouse species. We identify a high number of mucosa-associated bacterial taxa with significant heritability estimates, particularly for 16S rRNA transcript-based traits. Interestingly, heritability estimates also positively correlate with cospeciation rate estimates. Association mapping identifies 443 loci influencing 123 taxa, whose narrow genomic intervals enable promising individual candidate genes and pathways to be pinpointed. These results indicate a unique genetic architecture for cospeciating taxa, a clear enrichment for several classes of human disease, and identify important functional categories including innate immunity and G-protein-coupled receptors, whose role in host-microbe interactions diverge as new species form.

Keywords: microbiome; GWAS; cospeciation; codiversification; hybridization; phyllosymbiosis

Introduction

The recent widespread recognition of the gut microbiome's importance to host health and fitness represents a critical advancement of biomedicine. Host phenotypes affected by the gut microbiome are documented in humans (Ley et al., 2006; Turnbaugh et al., 2009; Lynch and Pedersen, 2016), laboratory animals (Backhed et al., 2004; Turnbaugh et al., 2008; Rolig et al., 2015; Rosshart et al., 2017; Gould et al., 2018), and wild populations (Suzuki, 2017; Roth et al., 2019; Suzuki et al., 2020; Hua et al., 2020), and include critical traits such as aiding digestion and energy uptake (Rowland et al., 2018) and the development and regulation of the immune system (Davenport, 2020).

Despite the importance of gut microbiome, community composition varies significantly among host species, populations, and individuals (Benson et al., 2010; Yatsunencko et al., 2012; Brooks et al., 2016; Rehman et al., 2016; Amato et al., 2019). While a portion of this variation is expected to be selectively neutral, alterations of the gut microbiome are on the one hand linked to numerous human diseases (Carding et al., 2015; Lynch and Pedersen, 2016) such as diabetes (Qin et al., 2012), inflammatory bowel disease (IBD) (Ott et al., 2004; Gevers et al., 2014) and mental disorders (Clapp et al., 2017). On the other hand, there is evidence that the gut microbiome can play an important role in adaptation on both recent- (Hehemann et al., 2010; Suzuki and Ley, 2020) and ancient evolutionary timescales (Rausch et al., 2019). Collectively, these phenomena suggest that it would be evolutionarily advantageous for hosts to influence their microbiome.

An intriguing observation made in comparative microbiome research in the last decade is that the pattern of diversification among gut microbiomes appears to mirror host phylogeny (Ochman et al., 2010). This phenomenon, coined "phylosymbiosis" (Brucker and Bordenstein, 2012a; Brucker and Bordenstein, 2012b), is documented in a number of diverse host taxa (Brooks et al., 2016) and also extends to the level of the phageome (Gogarten et al., 2021). Several non-mutually exclusive hypotheses are proposed to explain phylosymbiosis (Moran and Sloan, 2015). However, it is likely that vertical inheritance is important for at least a subset of taxa, as signatures of co-speciation/-diversification are present among numerous mammalian associated gut microbes (Moeller et al., 2016; Groussin et al., 2017; Moeller et al., 2019), which could also set the stage for potential coevolutionary processes. Importantly, experiments involving interspecific fecal microbiota transplants indeed provide evidence of host adaptation to their conspecific microbial communities (Brooks et al., 2016; Moeller et al., 2019). Further, cospeciating taxa were observed to be significantly enriched among the bacterial species depleted in early onset IBD, an immune-related disorder, suggesting a greater evolved dependency on such taxa (Papa et al., 2012; Groussin et al., 2017). However, the nature of genetic changes involving host-microbe interactions that take place as new host species diverge remains under-explored.

House mice are an excellent model system for evolutionary microbiome research, as

studies of both natural populations and laboratory experiments are possible (Suzuki, 2017; Suzuki et al., 2019). In particular, the house mouse species complex is comprised of subspecies that hybridize in nature, enabling the potential early stages of codiversification to be studied. We previously analyzed the gut microbiome across the central European hybrid zone of *Mus musculus musculus* and *M. m. domesticus* (Wang et al., 2015), which share a common ancestor ~ 0.5 million years ago (Geraldès et al., 2008). Importantly, transgressive phenotypes (i.e. exceeding or falling short of parental values) among gut microbial traits as well as increased intestinal histopathology scores were common in hybrids, suggesting that the genetic basis of host control over microbes has diverged (Wang et al., 2015). The same study performed an F₂ cross between wild-derived inbred strains of *M. m. domesticus* and *M. m. musculus* and identified 14 quantitative trait loci (QTL) influencing 29 microbial traits. However, like classical laboratory mice, these strains had a history of rederivation and reconstitution of their gut microbiome, thus leading to deviations from the native microbial populations found in nature (Rosshart et al., 2017; Org and Lüscher, 2018), and the genomic intervals were too large to identify individual genes.

In this study, we employed a powerful genetic mapping approach using inbred lines directly derived from the *M. m. musculus* - *M. m. domesticus* hybrid zone. Previous mapping studies using hybrids raised in a laboratory environment showed that high mapping resolution is possible due to the hundreds of generations of natural admixture between parental genomes in the hybrid zone (Turner and Harr, 2014; Pallares et al., 2014; Škrabar et al., 2018). Accordingly, we here identify 443 loci contributing to variation in 123 taxa, whose narrow genomic intervals (median <2Mb) enable many individual candidate genes and pathways to be pinpointed. We identify a high proportion of bacterial taxa with significant heritability estimates, and find that bacterial phenotyping based on 16S rRNA transcript compared to gene copy-based profiling yields an even higher proportion. Further, these heritability estimates also significantly positively correlate with cospeciation rate estimates, suggesting a more extensive host genetic architecture for cospeciating taxa. Finally, we identify numerous enriched functional pathways, whose role in host-microbe interactions may be particularly important as new species form.

Results

Microbial community composition

To obtain microbial traits for genetic mapping in the G2 mapping population, we sequenced the 16S rRNA gene from caecal mucosa samples of 320 hybrid male mice based on DNA and RNA (cDNA), which reflect bacterial cell number and activity, respectively. After applying quality filtering and subsampling 10,000 reads per sample, we identified a total of 4684 amplicon sequence variants (ASVs). For further analyses, we established a "core microbiome" (defined in Methods), such that analyses were limited to those taxa common and abundant enough to reveal potential genetic signal. The core microbiome is composed of four phyla, five classes, five orders, eleven families, 27 genera, and 90 ASVs for RNA, and four phyla, five classes, six orders, twelve families, 28 genera and 46 ASVs for DNA. A combined total of 98 unique ASVs belong to the core, of which 38 were shared between DNA and RNA (Suppl. Fig. 1). The most abundant genus in our core microbiome is *Helicobacter* (Suppl. Fig. 2), consistent with a previous study of the wild hybrid *M. m. musculus*/*M. m. domesticus* mucosa-associated microbiome (Wang et al., 2015).

Correlation between host genetic relatedness and microbiome structure

To gain a broad sense of the contribution of genetic factors to the variability of microbial phenotypes in our mapping population, we compared the kinship matrix based on genotypes to an equivalent based on gut microbial composition, whereby ASV abundances were used as equivalents of gene dosage. We found a significant correlation between these matrices ($P = .001$, $R^2=0.03$, Suppl. Fig. 3), indicating a host genetic effect on the diversity of the gut microbiota.

SNP-based heritability

Next, we used a SNP-based approach to estimate the proportion of variance explained (PVE) of the relative abundance of taxa, also called the narrow-sense heritability (h^2) or SNP-based heritability. Out of the 153 total core taxa, we identified 46 taxa for DNA and 69 taxa for RNA with significant heritability estimates ($P_{RLRT} < .05$), with estimates ranging between 29 and 91% (see Fig. 1A-B and Suppl. Table 1). An unclassified genus belonging to the phylum Bacteroidetes followed by ASV7 (genus *Paraprevotella*), *Paraprevotella* and Paraprevotellaceae showed the highest heritability among DNA-based traits (91.8%, 88.8%, 88.8%, and 87.1%, respectively; Fig. 1A), while ASV97 (genus *Oscillibacter*), followed by Prevotellaceae, *Paraprevotella* and ASV7 (*Paraprevotella*) had the highest heritability among RNA-based traits (86.6%, 85.7%, 85.7%, and 85.6%, resp.; Fig. 1B). The heritability estimates for DNA- and RNA-based measurements of the same taxa are significantly correlated ($P = 5.013 \times 10^{-8}$, $R^2=0.58$, Suppl. Fig. 4), and neither measure appears to be systematically more heritable than

another, i.e. some taxa display higher RNA-based heritability estimates and others higher DNA-based estimates.

Heritability estimates are correlated with predicted co-speciation rates

In an important meta-analysis of the gut microbiome across diverse mammalian taxa, Groussin et al. (2017) estimated co-speciation rates of individual bacterial taxa by measuring the congruence of host and bacteria phylogenetic trees relative to the number of host-swap events. We reasoned that taxa with higher co-speciation rates might also demonstrate higher heritability, as these more intimate evolutionary relationships would provide a greater opportunity for genetic aspects to evolve. Intriguingly, we observe a significant positive correlation for RNA-based traits ($P = .008$, $R^2 = .46$, Fig. 1D) and a similar trend for DNA ($P = 0.1$; Fig. 1C). These results support the notion that cospeciating taxa evolved a greater dependency on host genes, and further suggest that bacterial activity may better reflect the underlying biological interactions.

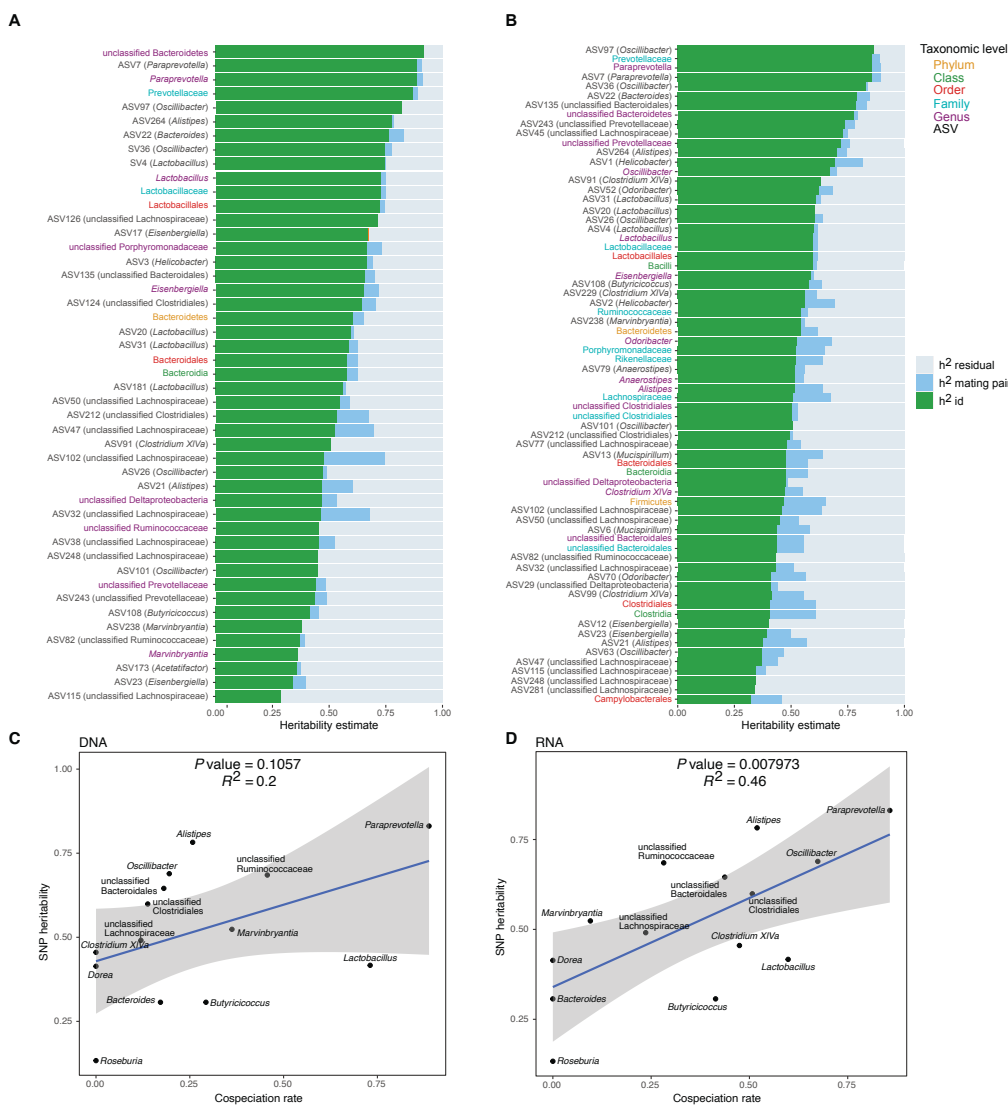


Figure 1: (A-B) Heritability estimates for the relative abundance of bacterial taxa. Proportion of variance explained for each taxon on DNA level (A), and RNA level (B) for all SNPs (GRM) in green, mating pair identifier in blue and residual variance in grey. Only significant heritability estimates are shown ($P < .05$). The text labels on the y-axis are colored according to taxonomic level: ASV in black, genus in purple, family in light blue, order in red, class in green, and phylum in yellow. (C-D) Relationship between the heritability estimates for the relative abundance of bacterial taxa and co-speciation rate for the same genus calculated by Groussin et al. (2017). DNA level (C), and RNA level (D). The blue line represents a linear regression fit to the data and the grey area the corresponding confidence interval.

Genetic mapping of host loci determining microbiome composition

Next, we performed genome-wide association mapping of the relative abundances of core taxa, in addition to two alpha-diversity measures (Shannon and Chao1 indices), based on 32,625 SNPs. We included both additive and dominance terms in the model to enable the identification of under- and over-dominance (see Methods). While we found no significant associations for alpha diversity at either the DNA or RNA level ($P > 1.53 \times 10^{-6}$), a total of 1099 genome-wide significant associations were identified for individual taxa ($P < 1.53 \times 10^{-6}$, Suppl. Table 2), of which 443 achieved study-wide significance ($P < 1.29 \times 10^{-8}$). Apart from the X chromosome, all autosomal chromosomes contained study-wide significant associations (Fig. 2A-B). Out of the 153 mapped taxa, 123 had at least one significant association (Table 1). For the remainder of our analyses, we focus on the results using the more stringent study-wide threshold, and combined significant SNPs within 10 Mb into significant regions (Suppl. Table 3). The median size of significant regions is 1.91 Mb, which harbor a median of 14 protein-coding genes. On average, we observe 10 significant mouse genomic regions per bacterial taxon.

Of the significant loci with estimated interval sizes, we find 73 intervals (16.5%) that are smaller than one Mb (Suppl. Table 4). The smallest interval is only 231 bases and associated with the RNA-based abundance of an unclassified genus belonging to Deltaproteobacteria. It is situated in an intron of the C3 gene, a complement component playing a central role in the activation of the complement system, which modulates inflammation and contributes to antimicrobial activity (Ricklin et al., 2016).

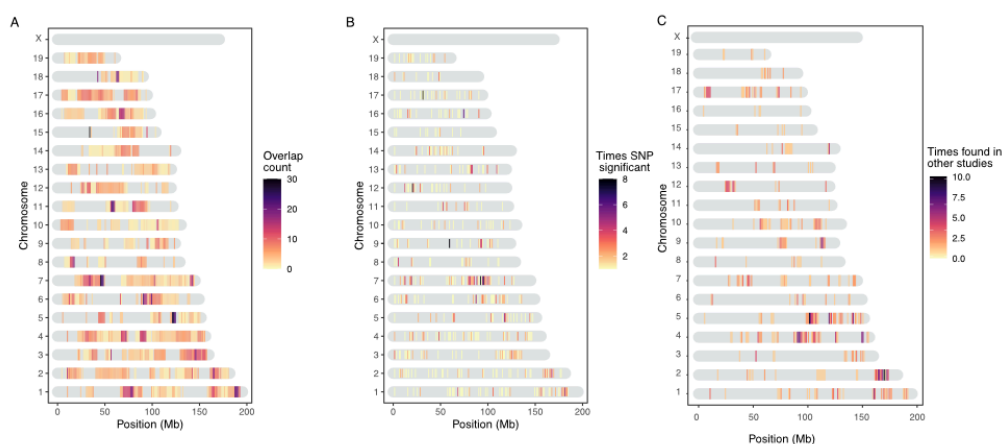


Figure 2: Heatmap of significant host loci from association mapping of bacterial abundances. Karotype plot showing the number of significant loci found using a study-wide threshold, where (A) plots the significance intervals, and (B) the significant SNP markers on the chromosomes. (C) shows the significant loci in this study that were previously found in other QTL studies of the mouse gut microbiome.

Table 1. Overview of mapping statistics.

	DNA	RNA	Total
Mapped taxa	101	142	153
Taxa with significant loci	67	96	123
Median interval size (Mb)	1.52	2.29	1.91
Total significant loci	478	791	1269
Unique significant loci	179	313	443
Significant loci total P	91	167	233
Significant loci additive P	155	260	377
Significant loci dominance P	95	166	231
Median significant loci per trait	5	6	8
Median unique significant loci per trait	3	3	4
Median unique significant SNPs per locus	2	2.5	2
Median number of genes per locus	31	52	43
Median protein coding genes per locus	11	15	14

The significant genomic regions and SNPs are displayed in Figure 2A and 3B, respectively. Individual SNPs were associated with up to 12 taxa, and significant intervals with up to 30 taxa. The SNPs with the lowest P values were associated with the genus *Dorea* and two ASVs belonging to *Dorea* (ASV184 and ASV293; Suppl. Fig. 5). At the RNA level this involves two loci: mm10-chr4: 67.07 Mb, where the peak SNP is 13 kb downstream of the closest gene *Tlr4* (UNC7414459, $P=2.31 \times 10^{-69}$, additive $P=4.48 \times 10^{-118}$, dominance $P=1.37 \times 10^{-111}$), and mm10-chr15: 94.4 Mb, where the peak SNP is found within the *Adams20* gene (UNC26145702, $P=4.51 \times 10^{-65}$, additive $P=1.87 \times 10^{-113}$, dominance $P=1.56 \times 10^{-105}$; Suppl. Fig. 5). Interestingly, the *Irak4* gene, whose protein

product is rapidly recruited after TLR4 activation, is also located 181 kb upstream of *Adamts20*. The five taxa displaying the most associations were ASV19 (*Bacteroides*), *Dorea*, ASV36 (*Oscillibacter*), ASV35 (*Bacteroides*), and ASV98 (unclassified Lachnospiraceae) (Suppl. Fig. 6).

Ancestry, dominance, and effect sizes

A total of 435 significant SNPs were ancestry informative between *M. m. musculus* and *M. m. domesticus* (i.e. represent fixed differences between subspecies). To gain further insight on the genetic architecture of microbial trait abundances, we estimated the degree of dominance at each significant locus using the d/a ratio (Falconer, 1996), where alleles with strictly recessive, additive, and dominant effects have d/a values of -1, 0, and 1, respectively. As half of the SNPs were not ancestry informative (Fig. 3A), it was not possible to consistently have a associated with one parent/subspecies, hence we report $d/|a|$ such that it can be interpreted with respect to bacterial abundance. For the vast majority of loci (83.53%), the allele associated with lower abundance is dominant or partially dominant ($-1.25 < d/|a| < -0.75$; Fig. 3B). On the basis of the arbitrary cutoffs we used to classify dominance, only a small proportion of alleles are underdominant (0.22%; $d/|a| < -1.25$) or overdominant (0.15%; $d/|a| > 1.25$). However for one-third of the significant SNPs, the heterozygotes display transgressive phenotypes, i.e. mean abundances that are either significantly lower (31% of SNPs)- or higher (2% of SNPs) than those of both homozygous genotypes. Interestingly, the *domesticus* allele was associated with higher bacterial abundance in two-thirds of this subset (33.2% vs 16.3% *musculus* allele; Fig. 3A).

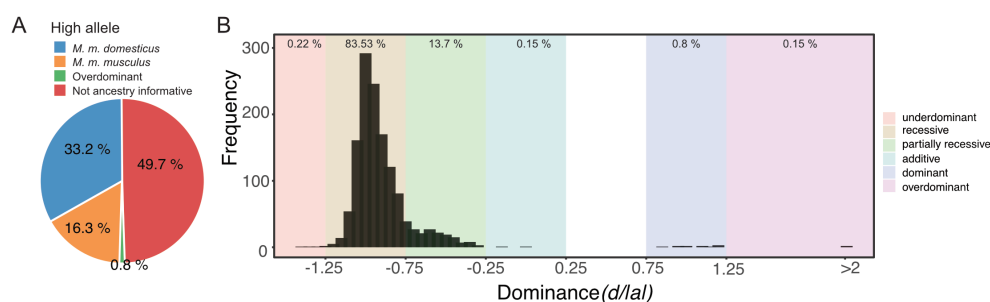


Figure 3: Genetic architecture of significant loci. A) Source of the allele with the highest phenotypic value. B) Histogram of dominance values d/a of significant loci reveals a majority of loci acting recessive or partially recessive.

Next, we estimated phenotypic effect sizes by calculating the percentage variance explained (PVE) by the peak SNP of each significant region. Peak SNPs explain between 3% and 64% of the variance in bacterial abundance, with a median effect size of 9.3% (Fig. 4A). The combined effects of all significant loci for each taxon ranged from 4.9% to 259%, with a median of 41.8% (Fig. 4B). Note, combined effects for many taxa (33 out of

59) exceed SNP-heritability estimates (Fig. 1). While exceeding 100% explained variance is biologically possible, as loci can have opposite phenotypic effects, many of these are likely inflated due to the Beavis effect (Beavis, 1994).

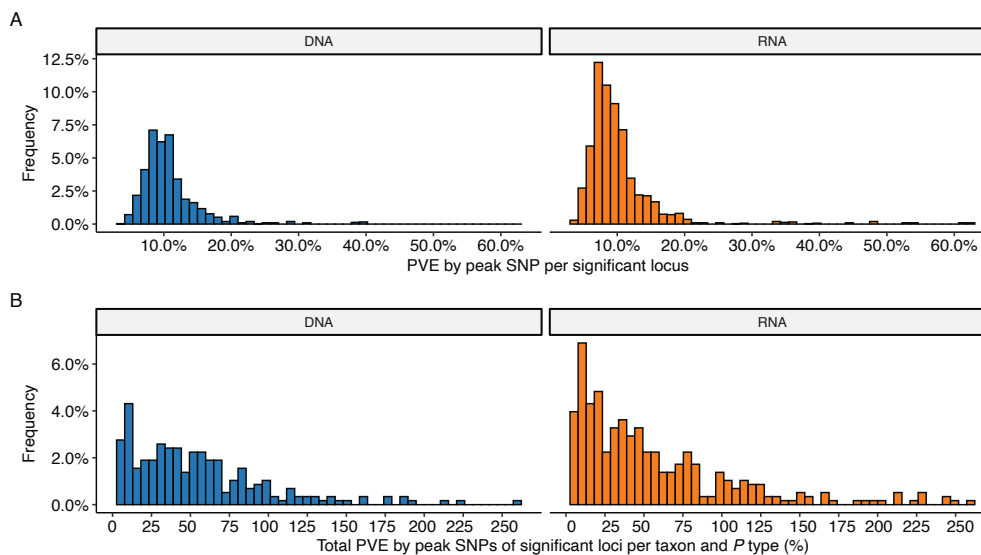


Figure 4: Effect sizes of loci significantly associated with bacterial abundances. (A) Histogram showing the percentage of variance explained (PVE) by the peak SNP for DNA (blue, left) and RNA (orange, right). (B) Collective PVE by lead SNPs of significant loci within a taxon. Values are calculated separately for each *P* value type (total, additive, and dominance).

Functional annotation of candidate genes

In order to reveal potential higher level biological phenomena among the identified loci, we performed pathway analysis to identify interactions and functional categories enriched among the genes in significant intervals. We used STRING (Szklarczyk et al., 2019) to calculate a protein-protein interaction (PPI) network of 925 protein-coding genes nearest to significant SNPs (upstream and downstream). A total of 768 genes were represented in the STRING database, and the maximal network is highly significant (PPI enrichment *P* value: 2.15×10^{-14}) displaying 668 nodes connected by 1797 edges and an average node degree of 4.68. After retaining only the edges with the highest confidence (interaction score > 0.9), this results in one large network with 233 nodes, 692 edges and ten smaller networks (Fig. 5).

Next, we functionally annotated clusters using STRING's functional enrichment plugin. The genes of the largest cluster are part of the G protein-coupled receptor (GPCR) ligand binding pathway. GPCRs are the largest receptor superfamily and also the largest class of drug targets (Sriram and Insel, 2018). We then calculated the top ten hub proteins from the network based on Maximal Clique Centrality (MCC) algorithm with CytoHubba to predict important nodes that can function as 'master switches' (Suppl. Fig. 7). The top ten proteins contributing to the PPI network were GNG12,

MCHR1, NMUR2, PROK2, OXTR, XCR1, TACR3, CHRM3, PTGFR, and C3, which are all involved in the GPCR signaling pathway.

Further, we performed enrichment analysis on the 925 closest genes using the *clusterprofiler* R package. We found 14 KEGG pathways to be over-represented: circadian entrainment, oxytocin signaling pathway, axon guidance, calcium signaling, cAMP signaling, cortisol synthesis and secretion, cushing syndrome, gastric acid secretion, glutamatergic synapse, mucin type O-glycan biosynthesis, inflammatory mediator regulation of TRP channels, PD-L1 expression and the PD-1 checkpoint pathway in cancer, tight junction, and the *Wnt* signaling pathway (Suppl. Table 5, Suppl. Fig. 8-9). Finally, genes involved in five human diseases are enriched, among them mental disorders (Suppl. Fig. 10).

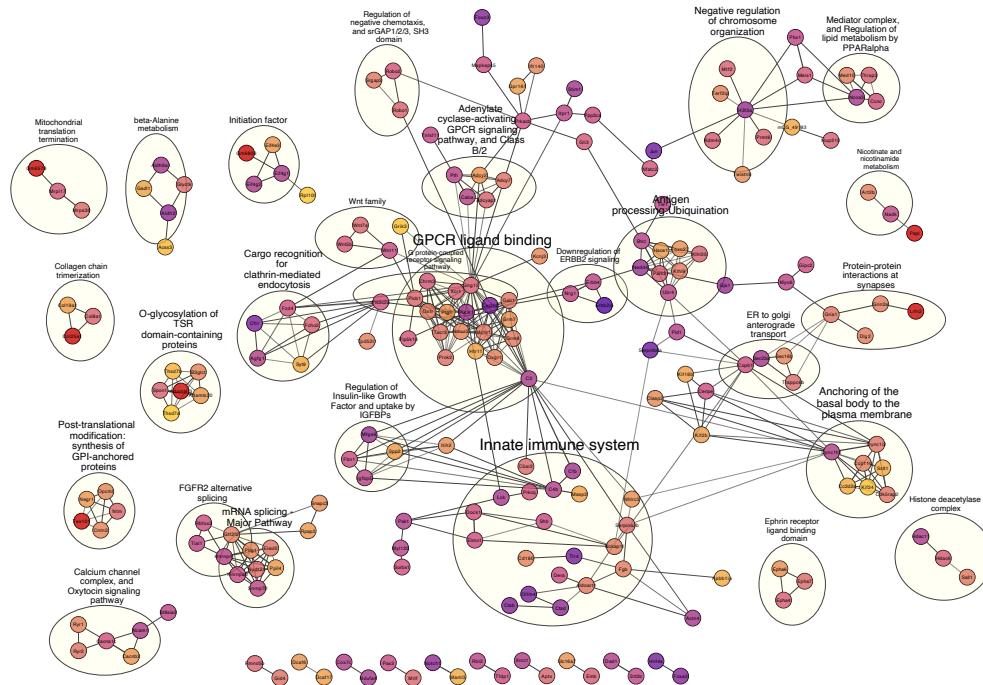


Figure 5: High confidence protein-protein interaction network of genes closest to SNPs significantly associated with bacterial abundances. Network clusters are annotated using STRING's functional enrichment (Doncheva et al., 2019). Nodes represent proteins and edges their respective interactions. Only edges with an interaction score higher than 0.9 are retained. The width of the edge line expresses the interaction score calculated by STRING. The color of the nodes describe the expression of the protein in the intestine where yellow is not expressed and purple is highly expressed.

Comparison of significant loci to published mouse gut microbiome studies

Next, we compiled a list of 648 unique confidence intervals of significant associations with gut bacterial taxa from seven previous mouse QTL studies (Benson et al., 2010; McKnite et al., 2012; Leamy et al., 2014; Wang et al., 2015; Org et al., 2015; Snijders et al., 2016; Kemis et al., 2019) and compared this list to our significance intervals for bacterial taxa at both the DNA and RNA level (346 unique intervals). Regions larger than 10Mb were removed from all studies. We found 434 overlapping intervals, which is significantly more than expected by chance (10 000 times permuted mean: 368, simulated $P=0.0073$, see Methods). Several of our smaller significant loci overlapped with larger loci from previous studies and removing this redundancy left 186 significant loci with a median interval size of 0.78 Mb (Fig. 2C). The most frequently identified locus is located on chromosome 2 169-171 Mb where protein coding genes *Gm11011*, *Znf217*, *Tshz2*, *Bcas1*, *Cyp24a1*, *Pfdn4*, *4930470P17Rik*, and *Dok5* are situated.

Proteins differentially expressed in germ-free vs conventional mice

To further validate our results, we compared the list of genes contained within intervals of our study to a list of differentially expressed protein between germ-free and conventionally raised mice (Mills et al., 2020). This comparison was made based on the general expectation that genes associated with variation in microbial abundances would be more likely to differ according to the colonization status of the host. Thus, we examined the intersection between genes identified in our study and the proteins identified as highly associated ($|\pi| > 1$) with the colonization state of the colon and the small intestine (Mills et al., 2020). Out of the 373 over- or under-expressed proteins according to colonization status, we find 198 of their coding genes to be among our significant loci, of which 17 are the closest genes to a significant marker (*Iyd*, *Nln*, *Slc26a3*, *Slc3a1*, *Myom2*, *Nebl*, *Tent5a*, *Fxr1*, *Cbr3*, *Chrodc1*, *Nucb2*, *Arhgef10l*, *Sucla2*, *Enpep*, *Prkcq*, *Aacs*, and *Cox7c*). This is significantly more than expected by chance (simulated $P=0.0156$, 10 000 permutations). Further, analyzing the protein-protein interactions with STRING results in a significant network ($P=1.73 \times 10^{-14}$, and average node degree 2.4, Suppl. Fig. 11), with *Cyp2c65*, *Cyp2c55*, *Cyp2b10*, *Gpx2*, *Cth*, *Eif3k*, *Eif1*, *Sucla2*, and *Rpl17* identified as hub genes (Suppl. Fig. 12).

Subsequently, we merged the information from Mills et al. (2020) and the seven previous QTL mapping studies discussed above to further narrow down the most promising candidate genes, and found 30 genes overlapping with our study. Of these 30 genes, six are the closest gene to a significant SNP. These genes are myomesine 2 (*Myom2*), solute carrier family 3 member 1 (*Slc3a1*), solute carrier family 26 member 3 (*Slc26a3*), nebulin (*Nebl*), carbonyl reductase 3 (*Cbr3*), and acetoacetyl-coA synthetase (*Aacs*).

STRING (<https://string-db.org>). The nodes represent proteins and are colored according to a selection of enriched GO terms and pathways: G protein coupled receptor (GPCR) signaling (red), regulation of the immune system process (blue), response to nutrient levels (light green), fatty acid metabolic process (pink), glucose homeostasis (purple), response to antibiotic (orange), regulation of feeding behavior (yellow), positive regulation of insulin secretion (dark green), circadian entrainment (brown), and response to vitamin D (turquoise). The color of the edges represents the interaction type: known interactions from curated databases (turquoise) or experimentally determined (pink); predicted interactions from gene neighborhood (green), gene fusions (red), gene co-occurrence (blue); other interactions from text-mining (light green), co-expression (black), and protein homology (purple).

Discussion

Understanding the forces that shape variation in host-associated bacterial communities within host species is key to understanding the evolution and maintenance of meta-organisms. Although numerous studies in mice and humans demonstrate that host genetics influences gut microbiota composition (McKnite et al., 2012; Leamy et al., 2014; Goodrich et al., 2014; Org et al., 2015; Davenport et al., 2015; Wang et al., 2016; Bonder et al., 2016; Goodrich et al., 2016; Kemis et al., 2019; Suzuki et al., 2019; Ishida et al., 2020; Hughes et al., 2020; Rühlemann et al., 2021), our study is unique in a number of important ways. First, the unique genetic resource of mice collected from a naturally occurring hybrid zone together with their native microbes yielded extremely high mapping resolution and the possibility to uncover ongoing evolutionary processes in nature. Second, our study is the first to perform genetic mapping of 16S rRNA transcripts in the gut environment, which was previously shown to be superior to DNA-based profiling in a genetic mapping study of the skin microbiota (Belheouane et al., 2017). Third, our study is one of the only to specifically examine the mucosa-associated community. It was previously reasoned that the mucosal environment may better reflect host genetic variation (Spor et al., 2011), and evidence for this hypothesis exists in nature (Linnenbrink et al., 2013). Finally, by cross-referencing our results with previous mapping studies and recently available proteomic data from germ-free versus conventional mice, we curated a more reliable list of candidate genes and pathways. Taken together, these results provide unique and unprecedented insight into the genetic basis for host-microbe interactions.

Importantly, by using wild-derived hybrid inbred strains to generate our mapping population, we gained insight into the evolutionary association between hosts and their microbiota at the transition from within species variation to between species divergence. Genetic relatedness in our mapping population significantly correlates with microbiome similarity, supporting a basis for codiversification at the early stages of speciation. A substantial proportion of microbial taxa are heritable, and heritability is correlated with cospeciation rates. This suggests that (i) vertical transmission could enable greater host adaptation to bacteria and/or (ii) the greater number of host genes associated with cospeciating taxa could indicate a greater dependency on the host, such that survival outside a specific host is reduced, making horizontal transmission less likely.

By performing 16S rRNA gene profiling at both the DNA and RNA level, we found that 30% (DNA-based) to 45% (RNA-based) of bacterial taxa are heritable, which is consistent with or higher than estimates reported in humans (~10%, Goodrich et al., 2016; ~21%, Turpin et al., 2016) and previous mouse studies (Kovacs et al., 2011; McKnite et al., 2012; Campbell et al., 2012; O'Connor et al., 2014; Carmody et al., 2015; Korach-Rechtman et al., 2019;). The high proportion of heritable taxa, with estimates of up to 91%, is likely explained in part by several factors of our study design. First, mice were

raised in a controlled common environment, and heritability estimates in other mammals were shown to be contingent on the environment (Grieneisen et al., 2021). Further, bacterial communities were sampled from cecal tissue instead of fecal content (Linnenbrink et al., 2013), and genetic variation was higher than in a typical mapping study due to subspecies differences. For the RNA-based traits, heritability estimates were significantly correlated with previously reported cospeciation rates in mammals (Groussin et al., 2017). This pattern, as well as the higher proportion of heritable taxa in RNA-based traits, suggest that host genetic effects are more strongly reflected by bacterial activity than cell number.

Accordingly, we found a total of 179 and 313 unique significant loci for DNA-based and RNA-based bacterial abundance, respectively, passing the conservative study-wide significance threshold. Taxa had a median of five significant loci, suggesting a complex and polygenic genetic architecture affecting bacterial abundances. We identify a higher number of loci in comparison to previous QTL and GWAS studies in mice (Benson et al., 2010; McKnite et al., 2012; Leamy et al., 2014; Wang et al., 2015; Org et al., 2015; Snijders et al., 2016; Kemis et al., 2019), which may be due to a number of factors. The parental strains of our study were never subjected to rederivation and subsequent reconstitution of their microbiota, and natural mouse gut microbiota are more variable than the artificial microbiota of laboratory strains (Kohl and Dearing, 2014; Weldon et al., 2015; Suzuki, 2017; Rosshart et al., 2017;). Furthermore, as noted above, our mapping population harbors both within- and between-subspecies genetic variation. We crossed incipient species sharing a common ancestor ~ 0.5 million years ago, hence we may also capture the effects of mutations that fixed rapidly between subspecies due to strong selection, which are typically not variable within species (Walsh, 1998; Barton and Keightley, 2002).

Importantly, our results also help to describe general features of the genetic architecture of bacterial taxon activity. For the majority of loci, the allele associated with lower relative abundance of the bacterial taxon was (partially) dominant. This suggests there is strong purifying selection against a high abundance of any particular taxon, which may help ensure high alpha diversity. The heterozygotes of one-third of significant SNPs displayed transgressive phenotypes. This is consistent with previous studies of hybrids (Turner et al., 2012; Turner and Harr, 2014; Wang et al., 2015;), for example, wild-caught hybrids showed broadly transgressive gut microbiome phenotypes. This pattern can be explained by over- or underdominance, or by epistasis (Rieseberg et al., 1999).

Notably, many loci significantly associated with bacterial abundance in this study were implicated in previous studies (Fig. 2C). For example, chromosome 2 169-171 Mb is associated with ASV23 (*Eisenbergiella*), *Eisenbergiella* and ASV32 (unclassified Lachnospiraceae) in this study, and overlaps with significant loci from three previous studies (Leamy et al., 2014; Snijders et al., 2016; Kemis et al., 2019). This region contains

eight protein-coding genes: *Gm11011*, *Znf217*, *Tshz2*, *Bcas1*, *Cyp24a1*, *Pfdn4*, *4930470P17Rik*, and *Dok5*. Another hotspot is on chromosome 5 101-103 Mb. This locus is significantly associated with four taxa in this study (Prevotellaceae, *Paraprevotella*, ASV7 genus *Paraprevotella* and *Acetatifactor*) and overlaps with associations for Clostridiales, Clostridiaceae, Lachnospiraceae, and Deferribacteriaceae (Snijders et al., 2016). Protein-coding genes in this region are: *Nkx6-1*, *Cds1*, *Wdfy3*, *Arhgap24*, and *Mapk10*. As previous studies were based on rederived mouse strains, identifying significant overlap in the identification of host loci suggests that some of the same genes and/or mechanisms influencing major members of gut microbial communities are conserved even in the face of community 'reset' in the context of re-derivation. The identity of the taxa is however not always the same, which suggests that functional redundancy may contribute to these observations, if *e.g.* several bacterial taxa fulfill the same function within the gut microbiome (Moya and Ferrer, 2016; Tian et al., 2020). Additionally, there is significant overlap of genes within loci identified in the current study and proteins differentially expressed in the intestine of germ-free mice compared to conventionally raised mice (Mills et al., 2020). Finally, by analyzing the functions of the genes closest to significant SNPs, we found that 12 of the 14 significantly enriched KEGG pathways were shown to be related to interactions with bacteria (Fonken et al., 2010; Thaïss et al., 2014; Neumann et al., 2014; Thaïss et al., 2015a; Thaïss et al., 2015b; Castoldi et al., 2015; Erdman and Poutahidis, 2016; Thaïss et al., 2016; Deaver et al., 2018; Wu et al., 2018; Peng et al., 2020; Nagpal et al., 2020; Hollander and Kaunitz, 2020; Suppl. Table 5).

To improve the robustness of our results, we combined multiple lines of evidence to prioritize candidates, resulting in a network of 80 genes (Suppl. Table 6). At the center of this network is a set of 22 proteins involved in G-protein coupled receptor signaling (Fig. 6, red nodes). MCHR1, NMUR2, and TACR3 (Fig. 6, yellow) are known to regulate feeding behavior (Saito et al., 1999; Cardoso et al., 2012; Smith et al., 2019), and CHRM3 to control digestion (Gautam et al., 2006; Tanahashi et al., 2009). Gut microbes can produce GPCR agonists to elicit host cellular responses (Cohen et al., 2017; Colosimo et al., 2019; Chen et al., 2019; Pandey et al., 2019). Thus, GPCRs may be key modulators of communication between the gut microbiota and host. Another interesting group of genes are those responding to nutrient levels (*Bmp7*, *Cd40*, *Aacs*, *Gclc*, *Nmur2*, *Cyp24a1*, *Adcyap1*, *Serpinc1*, and *Wnt11*) (Sethi and Vidal-Puig, 2008; Peier et al., 2009; Townsend et al., 2012; Yi and Bishop, 2015; Shi and Tu, 2015; Toderici et al., 2016; Yasuda et al., 2021; Gastelum et al., 2021;), as gut microbiota affect host nutrient uptake (Chung et al., 2018). In addition, CYP24A1, BMP7 and CD40 respond to vitamin D. Previous studies identified vitamin D/the vitamin D receptor to play a role in modulating the gut microbiota (Wang et al., 2016; Malaguarnera, 2020; Yang et al., 2020; Singh et al., 2020), and CD40 is known to induce a vitamin D dependent antimicrobial response through IFN- γ activation (Klug-Micu et al., 2013).

Another important category of candidate genes are those involved in immunity. Our most significant SNP was situated downstream of the *Tlr4* gene and was associated with the genus *Dorea* and several *Dorea* species. *Dorea* is a known short chain fatty acid producer (Taras et al., 2002; Reichardt et al., 2018) and interacts with tight junction proteins *Claudin-2* and *Occludin* (Alhasson et al., 2017). *Tlr4* is a member of the Toll-like receptor family, and has been linked with obesity, inflammation, and changes in the gut microbiota (Velloso et al., 2015). These combined results reflect an important role for *Dorea* in fatty acid harvesting and intestinal barrier integrity, both of which could act systemically to activate TLR4 and to promote metabolic inflammation (Cani et al., 2008; Delzenne et al., 2011; Nicholson et al., 2012). Moreover, the SNP with the second lowest *P* value was associated with the same taxa and situated 181 kb upstream of *Irak4*. IRAK4 is rapidly recruited after TLR4 activation to enable downstream activation of the NF κ B immune pathway. *Irak4* has previously been associated with a change in bacterial abundance using inbred mice (McKnite et al., 2012; Org et al., 2015).

Finally, we identified notable links between candidate genes and five human diseases (mental disorders, blood pressure finding, systemic arterial pressure, substance-related disorders, and atrial septal deficits; Suppl. Fig. 10). The connection to mental disorders is intriguing as involvement of the gut microbiota is suspected (Kelly et al., 2015; Foster et al., 2017; Cox and Weiner, 2018; Chen et al., 2019; Sarkar et al., 2020; Parker et al., 2020; Flux and Lowry, 2020). Taken together with our finding of an enriched set of GPCRs, this highlights the importance of host-microbial interplay along the gut-brain axis.

In summary, our study provides a number of novel insights into the importance of host genetic variation in shaping the gut microbiome, in particular for cospeciating bacterial taxa. These findings provide an exciting foundation for future studies of the precise mechanisms underlying host-gut microbiota interactions in the mammalian gut and should encourage future genetic mapping studies that extend analyses to the functional metagenomic sequence level.

Materials and Methods

Intercross design

We generated a mapping population using partially inbred strains derived from mice captured in the *M. m. musculus* - *M. m. domesticus* hybrid zone around Freising, Germany in 2008 (Turner et al., 2012). Originally, four breeding stocks were derived from 8-9 ancestors captured from one (FS, HA, TU) or two sampling sites (HO), and maintained with four breeding pairs per generation using the HAN-rotation outbreeding scheme (Rapp, 1972). Eight inbred lines (two per breeding stock) were generated by brother/sister mating of the 8th generation lab-bred mice. We set up the

cross when lines were at the 5th-9th generation of brother-sister meeting, with inbreeding coefficients of > 82%.

We first set up eight G1 crosses, each with one predominantly *domesticus* line (FS, HO - hybrid index <50%; see below) and one predominantly *musculus* line (HA, TU - hybrid index >50%); each line was represented as a dam in one cross and sire in another (Suppl. Fig. 14). One line, FS5, had a higher hybrid index than expected, suggesting there was a misidentification during breeding (see genotyping below). Next, we set up G2 crosses in eight combinations (subcrosses), such that each G2 individual has one grandparent from each of the initial four breeding stocks. We included 40 males from each subcross in the mapping population.

This study was performed according to approved animal protocols and institutional guidelines of the Max Planck Institute. Mice were maintained and handled in accordance with FELASA guidelines and German animal welfare law (Tierschutzgesetz § 11, permit from Veterinärämter Kreis Plön: 1401-144/PLÖ-004697).

Sample collection

Mice were sacrificed at 91 ± 5 days by CO₂ asphyxiation. We recorded body weight, body length and tail length, and collected ear tissue for genotyping. The caecum was removed and gently separated from its contents through bisection and immersion in RNAlater (Thermo Fisher Scientific, Schwerte, Germany). After overnight storage in RNAlater at 4° C, the RNAlater was removed and tissue stored at -20° C.

DNA extraction and sequencing

We simultaneously extracted DNA and RNA from caecum tissue samples using Qiagen (Hilden, Germany) Allprep DNA/RNA 96-well kits. We followed the manufacturer's protocol, with the addition of an initial bead beating step using Lysing matrix E tubes (MP Biomedical, Eschwege) to increase cell lysis. We used caecum tissue because host genetics has a greater influence on the microbiota at this mucosal site than on the lumen contents (Linnenbrink et al., 2013). We performed reverse transcription of RNA with High-Capacity cDNA Transcription Kits from Applied Biosystems (Darmstadt, Germany). We amplified the V1-V2 hypervariable region of the 16S rRNA gene using barcoded primers (27F-338R) with fused MiSeq adapters and heterogeneity spacers following (Rausch et al., 2016) and sequenced amplicons with 250 bp paired-reads on the Illumina MiSeq platform.

16S rRNA gene analysis

We assigned sequences to samples by exact matches of MID (multiplex identifier, 10 nt) sequences processed 16S rRNA sequences using the DADA2 pipeline, implemented in the DADA2 R package, version 1.16.0 (Callahan et al., 2016; Callahan, 2016). Briefly, raw sequences were trimmed and quality filtered with the maximum two 'expected errors' allowed in a read, paired sequences were merged and chimeras removed. For all

downstream analyses, we rarefied samples to 10,000 reads each. Due to the quality filtering, we have phenotyping data for 286 individuals on DNA level, and 320 G2 individuals on RNA level. We classified taxonomy using the Ribosomal Database Project (RDP) training set 16 (Cole et al., 2014). Classifications with low confidence at the genus level (<0.8) were grouped in the arbitrary taxon 'unclassified_group'.

We used the phyloseq R package (version 1.32.0) to estimate alpha diversity using the Shannon index and Chao1 index, and beta diversity using Bray-Curtis distance (McMurdie and Holmes, 2013). We defined core microbiomes at the DNA- and RNA-level, including taxa present in $> 25\%$ of the samples and with median abundance of non-zero values $> 0.2\%$ for amplicon sequence variant (ASV) and genus; and $>0.5\%$ for family, order, class and phylum.

Genotyping

We extracted genomic DNA from ear samples using Qiagen Blood and Tissue 96 well kits (Hilden, Germany), according to the manufacturer's protocol. We sent DNA samples from 26 G0 mice and 320 G2 mice to GeneSeek (Neogen, Lincoln, NE) for genotyping using the Giga Mouse Universal Genotyping Array (GigaMUGA; Morgan et al., 2015), an Illumina Infinium II array containing 141,090 single nucleotide polymorphism (SNP) probes. We quality-filtered genotype data using plink 1.9 (Chang et al., 2015); we removed individuals with call rates $<90\%$ and SNPs that were: not bi-allelic, missing in $>10\%$ individuals, with minor allele frequency $<5\%$, or Hardy-Weinberg equilibrium exact test P values $<1e-10$. A total of 64,103 SNPs and all but one G2 individual were retained. Prior to mapping, we LD-filtered SNPs with $r^2 >0.9$ using a window of 5 SNPs and a step size of 1 SNP. We retain 32,625 SNPs for mapping.

Hybrid index calculation

For each G0 and G2 mouse, we estimated a hybrid index – defined as the percentage of *M. m. musculus* ancestry. We identified ancestry-informative SNP markers by comparing GigaMUGA data from ten individuals each from two wild-derived outbred stocks of *M. m. musculus* (Kazakhstan and Czech Republic) and two of *M. m. domesticus* (Germany and France) maintained at the Max Planck Institute for Evolutionary Biology (L.M. Turner and B. Payseur, unpublished data). We classified SNPs as ancestry informative if they had a minimum of 10 calls per subspecies, the major allele differed between *musculus* and *domesticus*, and the allele frequency difference between subspecies was > 0.3 . A total of 48,361 quality-filtered SNPs from the G0/G2 genotype data were informative, including 8,775 SNPs with fixed differences between subspecies samples.

Correlation between host relatedness and microbiome structure

To investigate if host relatedness is correlated with individual variation in microbiome composition, we computed a centered relatedness matrix using the 32,625

filtered SNPs with GEMMA (v 0.98.1; Zhou and Stephens, 2012) and microbial composition-based kinship matrix among individuals based on relative bacterial abundances (Chen et al., 2018). The kinship matrix was calculated with the formula:

$$Kinship = 1/p \sum_{i=1}^p (x_i - 1_n \bar{x}_i)(x_i - 1_n \bar{x}_i)^T$$

where X denotes the $n \times p$ matrix of genotypes or relative abundances, x_i as its i th column representing the genotypes of i th SNP or the relative abundance of the i th ASV, \bar{x}_i as the sample mean and 1_n as a $n \times 1$ vector of 1's. We used a Mantel test with the Spearman's correlation to test for correlation between the host SNP-based kinship and microbial composition-based kinship using 10,000 permutations.

SNP-based heritability of microbial abundances

We calculated SNP-based heritabilities for bacterial abundances using a linear mixed model implemented in the lme4qtl R package (version 0.2.2; Ziyatdinov et al., 2018). The SNP-based heritability is expressed as:

$$h^2 = \frac{\sigma_g^2}{\sigma_g^2 + \sigma_m^2 + \sigma_e^2}$$

where σ_g^2 is the genetic variance estimated by K_{SNP} , σ_m^2 variance of the mating pair component, and σ_e^2 the variance due to residual environmental factors. We determined significance of the heritability estimates using exact likelihood ratio tests, following Supplementary Note 3 in Ziyatdinov et al., 2018, using the exactLRT() function of the R package RLRsim (version 3.1-6; Fabian et al., 2008).

Genome-wide association mapping

Prior to mapping, we inverse logistic transformed bacterial abundances using the inv.logit function from the R package gtools (version 3.9.2; Gregory R. Warnes, 2020).

We performed association mapping in the R package lme4qtl (version 0.2.2; Ziyatdinov et al., 2018) with the following linear mixed model:

$$y_i = \mu + a_i X_{ij}^a + d_i X_{ij}^d + Wu + e$$

where y_j is the phenotypic value of the j th individual; μ is the mean, X_{aij} the additive and X_{dij} the dominance genotypic index values coded as for individual j at locus i . a and d indicate fixed additive and dominance effects, W indicates random effects mating pair and kinship matrix, plus residual error e .

We estimated additive and dominance effects separately because we expected to observe underdominance and overdominance in our hybrid mapping population, as well as additive effects, and aimed to estimate their relative importance. To model the

additive effect (i.e. 1/2 distance between homozygous means), genotypes at each locus, i , were assigned additive index values ($X^a \in \{1, 0, -1\}$) for AA, AB, BB, respectively, with A indicating the major allele and B the minor allele. To model dominance effects (i.e. heterozygote mean - midpoint of homozygote means), genotypes were assigned dominance index values ($X^d \in \{0, 1\}$) for homozygotes and heterozygotes, respectively.

We included mating pair as a random effect to account for maternal effects and cage effects, as male litter mates are kept together in a cage after weaning. We included kinship coefficient as a random effect in the model to account for population and family structure. To avoid proximal contamination, we used a leave-one-chromosome-out approach, that is, when testing each single-SNP association we used a relatedness matrix omitting markers from the same chromosome (Parker et al., 2014). Hence, for testing SNPs on each chromosome, we calculated a centered relatedness matrix using SNPs from all other chromosomes with GEMMA (v0.97; Zhou and Stephens, 2012). We calculated P values for single-SNP associations by comparing the full model to a null model excluding fixed effects. Code for performing the mapping is available at https://github.com/sdoms/mapping_scripts.

We evaluated significance of SNP-trait associations using two thresholds; first, we used a genome-wide threshold for each trait, where we corrected for multiple testing across markers using the Bonferroni method (Abdi, 2007). Second, as bacteria interact with each other within the gut as members of a community, bacterial abundances are non-independent, so we calculated a study-wide threshold dividing the genome-wide threshold by the number of effective taxa included. We used matSpDLite (Nyholt, 2019; Li and Ji, 2005; Qin et al., 2020) to estimate the number of effective bacterial taxa based on eigenvalue variance.

To estimate the genomic interval represented by each significant LD-filtered SNP, we report significant regions defined by the most distant flanking SNPs in the full pre-LD-filtered genotype dataset showing $r^2 > 0.9$ with each significant SNP. We combined significant regions less than 10 Mb apart into a single region. Genes situated in significant regions were retrieved using biomaRt (Steffen Durinck, 2009), and the mm10 mouse genome.

Dominance analyses

We classified dominance for SNPs with significant associations on the basis of the d/a ratio (Falconer, 1996) where d is the dominance effect, a the additive effect. As the expected value under purely additive effects is 0. As our mapping population is a multi-parental-line cross, and not all SNPs were ancestry-informative with respect to *musculus/domesticus*, the sign of a effects is defined by the major allele within our mapping population, which lacks clear biological interpretation. To provide more meaningful values, we report $d/|a|$, such that a value of 1 = complete dominance of the allele associated with higher bacterial abundance, and a value of -1 = complete dominance of

the allele associated with lower bacterial abundance. Values above 1 or below -1 indicate over/underdominance. We classified effects of significant regions the following arbitrary $d/|a|$ ranges to classify dominance of significant regions (Burke et al., 2002; Miller et al., 2014): underdominant <-1.25 , high abundance allele recessive between -1.25 and -0.75, partially recessive between -0.75 and -0.25, additive between -0.25 and 0.25, partially dominant between 0.25 and 0.75, dominant 0.75 and 1.25, and overdominant >1.25 .

Gene ontology and network analysis

The nearest genes up- and downstream of the significant SNPs were identified using the `locateVariants()` function from the VariantAnnotation R package (version 1.34.0; Valerie et al., 2014) using the default parameters. A maximum of two genes per locus were included (one upstream, and one downstream of a given SNP).

To investigate functions and interactions of candidate genes, we calculated a a protein-protein interaction (PPI) network with STRING version 11 (Szklarczyk et al., 2019), on the basis of a list of the closest genes to all SNPs with significant trait associations. We included network edges with an interaction score >0.9 , based on evidence from fusion, neighborhood, co-occurrence, experimental, text-mining, database, and co-expression. We exported this network to Cytoscape v 3.8.2 (Shannon et al., 2003) for identification of highly interconnected regions using the MCODE Cytoscape plugin (Bader and Hogue, 2003), and functional annotation of clusters using the `stringApp` Cytoscape plugin (Doncheva et al., 2019).

We identified overrepresented KEGG pathways and human diseases using the `clusterProfiler` R package (version 3.16.1; Yu et al., 2012). P values were corrected for multiple testing using the Benjamini-Hochberg method. Pathways and diseases with an adjusted P value $< .05$ were considered over-represented.

Calculating overlap with other studies

To test for significant overlap with loci identified in previous mapping studies, we used the tool `poverlap` (Brent Pedersen, 2013) to compare observed overlap to random expectations based on 10,000 permutations of significant regions. We identified genes within overlapping regions using the `locateVariants()` function from the VariantAnnotation R package (version 1.34.0; Valerie et al., 2014).

Combination of results

Hub genes SNP network and their first neighbors, the hub genes from the 'differentially expressed in GF mice'-network and their respective first neighbors, genes found in both Mills et al. (2020) and other mouse QTL studies, closest genes to a SNP found in Mills et al. (2020), genes situated in the 20 smallest intervals, six genes in the two intervals with the lowest P values, twenty genes in intervals found in most different taxa, genes situated in the region with most overlap within our study, and finally the

genes situated in the intervals that most frequently overlapped with other studies were combined into one gene set and analyzed with STRING. Genes situated in the same genomic locus were curated according to the number of edges in the STRING network.

Data and code availability: DNA- and RNA-based 16S rRNA gene sequences are available under project accession number PRJNA759194. Code is available at https://github.com/sdoms/mapping_scripts.

Supplementary Materials: Suppl. Fig 1-14, Table S1: Heritability estimates, Table S2: Genome-wide significant associations, Table S3: Study-wide significant associations, Table S4: Intervals smaller than 1Mb, Table S5: Overrepresented KEGG pathways, Table S6: Candidate genes.

Acknowledgments: We thank Diethard Tautz for generous support of mouse breeding and Camilo Medina and the MPI-Plön mouse team for performing mouse husbandry, and Katja Cloppenborg-Schmidt and Dr. Sven Künzel for their excellent technical assistance. We thank Mathieu Groussin for assistance with cospeciation rate data. Research funding for this project was provided by the Deutsche Forschungsgemeinschaft Collaborative Research Center 1182, 'Origin and Function of Metaorganisms' (J.F.B. and A.F.) and TU 500/2-1 to L.M.T, and by the Max Planck Society (to D. Tautz).

Author contributions: Conceptualization: L.M.T., S.I., and J.F.B; Methodology: L.M.T, J.F.B., S.D., S.I., and A.K.; Software: S.D., M.R., and L.M.T; Validation: S.D., M.R., A.K., and L.M.T; Formal Analysis: S.D., M.R., A.K., and L.M.T; Investigation: S.D. and L.M.T; Resources: S.D., H.F., and C.C; Writing - Original Draft: S.D.; Writing - Review & Editing: S.D., L.M.T, and J.F.B; Visualization: S.D. and L.M.T; Supervision: L.M.T., A.F., and J.F.B.; Project Administration: J.F.B.; Funding Acquisition: A.F., L.M.T, and J.F.B.

Conflicts of Interest: The authors declare no conflict of interest.

References

- Abdi, Hervé (2007), 'The Bonferonni and Šidák Corrections for Multiple Comparisons', in Salkind, Neil J. (ed.), (Encyclopedia of Measurement and Statistics, SAGE), 9.
- Alhasson, Firas, et al. (2017), 'Altered gut microbiome in a mouse model of Gulf War Illness causes neuroinflammation and intestinal injury via leaky gut and TLR4 activation', *PLoS One*, 12 (3), e0172914.
- Amato, Katherine R, et al. (2019), 'Evolutionary trends in host physiology outweigh dietary niche in structuring primate gut microbiomes', *The ISME journal*, 13 (3), 576-87.
- Backhed, F., et al. (2004), 'The gut microbiota as an environmental factor that regulates fat storage', *Proceedings of the National Academy of Sciences*, 101 (44), 15718-23.
- Bader, Gary D. and Christopher WV Hogue (2003), 'An automated method for finding molecular complexes in large protein interaction networks', *BMC Bioinformatics*, 4 (1), 2.
- Barton, Nicholas H. and Peter D. Keightley (2002), 'Understanding quantitative genetic variation', *Nat. Rev. Genet.*, 3 (1), 11-21.
- Beavis, WD (1994), 'The power and deceit of QTL experiments: lessons from comparative QTL studies', Proceedings of the forty-ninth annual corn and sorghum industry research conference 250 266.
- Belheouane, Meriem, et al. (2017), 'Improved detection of gene-microbe interactions in the mouse skin microbiota using high-resolution QTL mapping of 16S rRNA transcripts', *Microbiome*, 5 (1), 1-17.
- Benson, Andrew K., et al. (2010), 'Individuality in gut microbiota composition is a complex polygenic trait shaped by multiple environmental and host genetic factors', *Proceedings of the National Academy of Sciences of the United States of America*
Proc. Natl. Acad. Sci. U.S.A., 107 (44), 18933-38.
- Bonder, Marc Jan, et al. (2016), 'The effect of host genetics on the gut microbiome', *Nat. Genet.*, 48 (11), 1407-12.
- Brent Pedersen, Joe Brown (2013), 'poverlap: significance testing over interval overlaps',
- Brooks, AW, et al. (2016), 'Phylosymbiosis: Relationships and Functional Effects of Microbial Communities across Host Evolutionary History.', *PLoS Biol.*, 14 (11), e2000225.
- Brucker, RM and SR Bordenstein (2012a), 'Speciation by symbiosis.', *Trends Ecol Evol*, 27 (8), 443-51.
- Brucker, Robert M and Seth R Bordenstein (2012b), 'The roles of host evolutionary relationships (genus: Nasonia) and development in structuring microbial communities', *Evolution: International Journal of Organic Evolution*, 66 (2), 349-62.
- Burke, John M., et al. (2002), 'Genetic Analysis of Sunflower Domestication', *Genetics*, 161 (3), 1257-67.
- Callahan, Benjamin J (2016), 'DADA2 pipeline', *DADA2*,
- Callahan, Benjamin J, et al. (2016), 'DADA2: High resolution sample inference from Illumina amplicon data', *Nature methods*
Nat Methods, 13 (7), 581-83.
- Campbell, JH, et al. (2012), 'Host genetic and environmental effects on mouse intestinal microbiota.', *ISME J*, 6 (11), 2033-44.
- Cani, Patrice D., et al. (2008), 'Changes in gut microbiota control metabolic endotoxemia-induced inflammation in high-fat diet-induced obesity and diabetes in mice', *Diabetes*, 57 (6), 1470-81.
- Carding, Simon, et al. (2015), 'Dysbiosis of the gut microbiota in disease', *Microb. Ecol. Health Dis.*, 26
- Cardoso, JC, et al. (2012), 'Feeding and the rhodopsin family g-protein coupled receptors in nematodes and arthropods.', *Front Endocrinol (Lausanne)*, 3 157.
- Carmody, RN, et al. (2015), 'Diet dominates host genotype in shaping the murine gut microbiota.', *Cell Host Microbe*, 17 (1), 72-84.
- Castoldi, Angela, et al. (2015), 'They Must Hold Tight: Junction Proteins, Microbiota And Immunity In Intestinal Mucosa', *Current Protein & Peptide Science*
Curr Protein Pept Sci, 16 (7), 655-71.
- Chang, Christopher C, et al. (2015), 'Second-generation PLINK: rising to the challenge of larger and richer datasets', *GigaScience*
GigaSci, 4 (1), 7.
- Chen, Congying, et al. (2018), 'Contribution of Host Genetics to the Variation of Microbial Composition of Cecum Lumen and Feces in Pigs', *Frontiers in Microbiology*

Front. Microbiol., 9

Chen, Haiwei, et al. (2019), 'A forward chemical genetic screen reveals gut microbiota metabolites that modulate host physiology', *Cell*, 177 (5), 1217-1231.e18.

Chung, HJ, et al. (2018), 'Gut Microbiota as a Missing Link Between Nutrients and Traits of Human.', *Front Microbiol*, 9 1510.

Clapp, M, et al. (2017), 'Gut microbiota's effect on mental health: The gut-brain axis.', *Clin Pract*, 7 (4), 987.

Cohen, Louis J., et al. (2017), 'Commensal bacteria make GPCR ligands that mimic human signalling molecules', *Nature*, 549 (7670), 48-53.

Cole, JR, et al. (2014), 'Ribosomal Database Project: data and tools for high throughput rRNA analysis.', *Nucleic Acids Res.*, 42 (Database issue), D633-42.

Colosimo, Dominic A., et al. (2019), 'Mapping Interactions of Microbial Metabolites with Human G-Protein-Coupled Receptors', *Cell Host & Microbe*, 26 (2), 273-282.e7.

Cox, Laura M. and Howard L. Weiner (2018), 'Microbiota Signaling Pathways that Influence Neurologic Disease', *Neurotherapeutics*, 15 (1), 135-45.

Davenport, Emily R., et al. (2015), 'Genome-Wide Association Studies of the Human Gut Microbiota', *PLoS One*, 10 (11), e0140301.

Davenport, Emily R. (2020), 'Genetic Variation Shapes Murine Gut Microbiota via Immunity', *Trends in Immunology*, 41 (1), 1-3.

Deaver, Jessica A., Sung Y. Eum, and Michal Toborek (2018), 'Circadian Disruption Changes Gut Microbiome Taxa and Functional Gene Composition', *Frontiers in Microbiology*

Front Microbiol, 9 737.

Delzenne, Nathalie M., et al. (2011), 'Targeting gut microbiota in obesity: effects of prebiotics and probiotics', *Nature Reviews. Endocrinology*

Nat Rev Endocrinol, 7 (11), 639-46.

Doncheva, Nadezhda T., et al. (2019), 'Cytoscape StringApp: Network Analysis and Visualization of Proteomics Data', *Journal of Proteome Research*

J Proteome Res, 18 (2), 623-32.

Erdman, S.E. and T. Poutahidis (2016), 'Microbes and Oxytocin', *131* (Int. Rev. Neurobiol., Elsevier), 91-126.

Fabian, Scheipl, Greven Sonja, and Kuechenhoff Helmut (2008), 'Size and power of tests for a zero random effect variance or polynomial regression in additive and linear mixed models.', *Computational Statistics & Data Analysis*, 52 (7), 3283-99.

Falconer, D. S (1996), *Introduction to quantitative genetics*, (Harlow, England: Prentice Hall).

Flux, M. C. and Christopher A. Lowry (2020), 'Finding intestinal fortitude: Integrating the microbiome into a holistic view of depression mechanisms, treatment, and resilience', *Neurobiology of Disease*

Microbiome in neurological and psychiatric disease

Neurobiology of Disease, 135 104578.

Fonken, Laura K., et al. (2010), 'Light at night increases body mass by shifting the time of food intake', *Proceedings of the National Academy of Sciences*

PNAS, 107 (43), 18664-69.

Foster, Jane A., Linda Rinaman, and John F. Cryan (2017), 'Stress & the gut-brain axis: Regulation by the microbiome', *Neurobiology of Stress*, 7 124-36.

Gastelum, C, et al. (2021), 'Adaptive Changes in the Central Control of Energy Homeostasis Occur in Response to Variations in Energy Status.', *Int J Mol Sci*, 22 (5), 2728.

Gautam, D, et al. (2006), 'A critical role for beta cell M3 muscarinic acetylcholine receptors in regulating insulin release and blood glucose homeostasis in vivo.', *Cell Metab*, 3 (6), 449-61.

Geraldes, A, et al. (2008), 'Inferring the history of speciation in house mice from autosomal, X-linked, Y-linked and mitochondrial genes.', *Mol Ecol*, 17 (24), 5349-63.

Gevers, Dirk, et al. (2014), 'The treatment-naive microbiome in new-onset Crohn's disease', *Cell host & microbe*, 15 (3), 382-92.

Gogarten, Jan F, et al. (2021), 'Primate phageomes are structured by superhost phylogeny and environment', *Proceedings of the National Academy of Sciences*, 118 (15),

Goodrich, Julia K., et al. (2014), 'Human genetics shape the gut microbiome', *Cell*, 159 (4), 789-99.

- Goodrich, Julia K., et al. (2016), 'Genetic Determinants of the Gut Microbiome in UK Twins', *Cell host & microbe*,
- Gould, AL, et al. (2018), 'Microbiome interactions shape host fitness.', *Proc. Natl. Acad. Sci. U S A*, 115 (51), E11951-60.
- Gregory R. Warnes, Ben Bolker and Thomas Lumley (2020), 'gtools: Various R Programming Tools',
- Grieneisen, L, et al. (2021), 'Gut microbiome heritability is nearly universal but environmentally contingent.', *Science*, 373 (6551), 181-86.
- Groussin, Mathieu, et al. (2017), 'Unraveling the processes shaping mammalian gut microbiomes over evolutionary time', *Nature Comm.*, 8 (1), 14319.
- Hehemann, Jan-Hendrik, et al. (2010), 'Transfer of carbohydrate-active enzymes from marine bacteria to Japanese gut microbiota', *Nature*, 464 (7290), 908-12.
- Hollander, Daniel and Jonathan D. Kaunitz (2020), 'The "Leaky Gut": Tight Junctions but Loose Associations', *Digestive Diseases and Sciences*
- Dig Dis Sci*, 65 (5), 1277-87.
- Hua, Yan, et al. (2020), 'Gut microbiota and fecal metabolites in captive and wild North China leopard (*Panthera pardus japonensis*) by comparison using 16 s rRNA gene sequencing and LC/MS-based metabolomics', *BMC Veterinary Research*, 16 (1),
- Hughes, David A., et al. (2020), 'Genome-wide associations of human gut microbiome variation and implications for causal inference analyses', *Nature Microbiology*, 5 (9), 1079-87.
- Ishida, Sachiko, et al. (2020), 'Genome-wide association studies and heritability analysis reveal the involvement of host genetics in the Japanese gut microbiota', *Communications Biology*
- Commun Biol*, 3
- Kelly, John R., et al. (2015), 'Breaking Down the Barriers: The Gut Microbiome, Intestinal Permeability and Stress-related Psychiatric Disorders', *Frontiers in Cellular Neuroscience*
- Front. Cell. Neurosci.*, 9
- Kemis, Julia H., et al. (2019), 'Genetic determinants of gut microbiota composition and bile acid profiles in mice', *PLoS Genet.*, 15 (8), e1008073.
- Klug-Micu, GM, et al. (2013), 'CD40 ligand and interferon- γ induce an antimicrobial response against *Mycobacterium tuberculosis* in human monocytes.', *Immunology*, 139 (1), 121-28.
- Kohl, KD and MD Dearing (2014), 'Wild-caught rodents retain a majority of their natural gut microbiota upon entrance into captivity.', *Environ Microbiol Rep*, 6 (2), 191-95.
- Korach-Rechtman, H, et al. (2019), 'Murine Genetic Background Has a Stronger Impact on the Composition of the Gut Microbiota than Maternal Inoculation or Exposure to Unlike Exogenous Microbiota.', *Appl. Environ. Microbiol.*, 85 (18), e00826-19.
- Kovacs, Amir, et al. (2011), 'Genotype is a stronger determinant than sex of the mouse gut microbiota', *Microbial ecology*, 61 (2), 423-28.
- Leamy, Larry J, et al. (2014), 'Host genetics and diet, but not immunoglobulin A expression, converge to shape compositional features of the gut microbiome in an advanced intercross population of mice', *Genome Biology*
- Genome Biol*, 15 (12),
- Ley, RE, et al. (2006), 'Microbial ecology: human gut microbes associated with obesity.', *Nature*, 444 (7122), 1022-23.
- Li, J. and L. Ji (2005), 'Adjusting multiple testing in multilocus analyses using the eigenvalues of a correlation matrix', *Heredity*, 95 (3), 221-27.
- Linnenbrink, Miriam, et al. (2013), 'The role of biogeography in shaping diversity of the intestinal microbiota in house mice', *Molecular Ecology*, 22 (7), 1904-16.
- Lynch, SV and O Pedersen (2016), 'The Human Intestinal Microbiome in Health and Disease.', *N. Engl. J. Med.*, 375 (24), 2369-79.
- Malaguarrera, L (2020), 'Vitamin D and microbiota: Two sides of the same coin in the immunomodulatory aspects.', *Int Immunopharmacol*, 79 106112.
- McKnite, Autumn M., et al. (2012), 'Murine Gut Microbiota Is Defined by Host Genetics and Modulates Variation of Metabolic Traits', *PLoS One*, 7 (6),
- McMurdie, Paul J and Susan Holmes (2013), 'phyloseq: an R package for reproducible interactive analysis and graphics of microbiome census data', *PLoS One*, 8 (4), e61217.
- Walsh, Michael Lynch and Bruce (1998), *Genetics and Analysis of Quantitative Traits*, (Sunderland, MA: Sinauer).
- Miller, Craig T., et al. (2014), 'Modular Skeletal Evolution in Sticklebacks Is Controlled by Additive and Clustered Quantitative Trait Loci', *Genetics*, 197 (1), 405-20.
- Mills, Robert H., et al. (2020), 'Organ-level protein networks as a reference for the host effects of the microbiome',

Genome Research

Genome Res., 30 (2), 276-86.

Moeller, Andrew H., et al. (2016), 'Cospeciation of gut microbiota with hominids', *Science (New York, N.Y.)*

Science, 353 (6297), 380-82.

Moeller, Andrew H., et al. (2019), 'Experimental Evidence for Adaptation to Species-Specific Gut Microbiota in House Mice', *mSphere*, 4

Moran, Nancy A. and Daniel B. Sloan (2015), 'The Hologenome Concept: Helpful or Hollow', *PLoS Biol.*, 13 (12), e1002311.

Morgan, Andrew P., et al. (2015), 'The Mouse Universal Genotyping Array: From Substrains to Subspecies', *G3: GenesGenomesGenetics*

G3 (Bethesda), 6 (2), 263-79.

Moya, Andrés and Manuel Ferrer (2016), 'Functional Redundancy-Induced Stability of Gut Microbiota Subjected to Disturbance', *Trends Microbiol.*, 24 (5), 402-13.

Nagpal, Ravinder, et al. (2020), 'Role of TRP Channels in Shaping the Gut Microbiome', *Pathogens*, 9

Neumann, Philipp-Alexander, et al. (2014), 'Gut Commensal Bacteria and Regional Wnt Gene Expression in the Proximal Versus Distal Colon', *The American Journal of Pathology*

Am J Pathol, 184 (3), 592-99.

Nicholson, Jeremy K., et al. (2012), 'Host-gut microbiota metabolic interactions', *Science (New York, N.Y.)*

Science, 336 (6086), 1262-67.

Nyholt, Dale R. (2019), 'matSpD local version - Statistical and Genomic Epidemiology Laboratory (SGEL)',

O'Connor, Annalouise, et al. (2014), 'Responsiveness of cardiometabolic-related microbiota to diet is influenced by host genetics', *Mammalian Genome*, 25 (11), 583-99.

Ochman, Howard, et al. (2010), 'Evolutionary relationships of wild hominids recapitulated by gut microbial communities', *PLoS Biol.*, 8 (11), e1000546.

Org, Elin, et al. (2015), 'Genetic and environmental control of host-gut microbiota interactions', *Genome Research*

Genome Res., 25 (10), 1558-69.

Org, Elin and Aldons J. Lusic (2018), 'Using the natural variation of mouse populations to understand host-gut microbiome interactions', *Drug discovery today. Disease models*

Drug Discov Today Dis Models, 28 61-71.

Ott, SJ, et al. (2004), 'Reduction in diversity of the colonic mucosa associated bacterial microflora in patients with active inflammatory bowel disease', *Gut*, 53 (5), 685-93.

Pallares, LF, et al. (2014), 'Use of a natural hybrid zone for genomewide association mapping of craniofacial traits in the house mouse.', *Mol Ecol*, 23 5756-70.

Pandey, Shubhi, Jagannath Maharana, and Arun K. Shukla (2019), 'The Gut Feeling: GPCRs Enlighten the Way', *Cell Host & Microbe*, 26 (2), 160-62.

Papa, Eliseo, et al. (2012), 'Non-invasive mapping of the gastrointestinal microbiota identifies children with inflammatory bowel disease', *PLoS One*, 7 (6), e39242.

Parker, Bianca J., et al. (2020), 'The Genus *Alistipes*: Gut Bacteria With Emerging Implications to Inflammation, Cancer, and Mental Health', *Frontiers in Immunology*

Front. Immunol., 11

Parker, CC, et al. (2014), 'High-resolution genetic mapping of complex traits from a combined analysis of F2 and advanced intercross mice.', *Genetics*, 198 (1), 103-16.

Peier, Andrea, et al. (2009), 'The Antiobesity Effects of Centrally Administered Neuromedin U and Neuromedin S Are Mediated Predominantly by the Neuromedin U Receptor 2 (NMUR2)', *Endocrinology*, 150 (7), 3101-9.

Peng, Zhi, et al. (2020), 'The Gut Microbiome Is Associated with Clinical Response to Anti-PD-1/PD-L1 Immunotherapy in Gastrointestinal Cancer', *Cancer Immunology Research*

Cancer Immunol Res, 8 (10), 1251-61.

Qin, Junjie, et al. (2012), 'A metagenome-wide association study of gut microbiota in type 2 diabetes', *Nature*, 490 (7418), 55-60.

Qin, Youwen, et al. (2020), 'Combined effects of host genetics and diet on human gut microbiota and incident disease in a single population cohort',

- Rapp, K (1972), 'HAN-rotation, a new system for rigorous outbreeding', *Z. Versuchstierk.*, 14 133-42.
- Rausch, P, et al. (2016), 'Analysis of factors contributing to variation in the C57BL/6J fecal microbiota across German animal facilities.', *Int. J. Med. Microbiol.*, 306 (5), 343-55.
- Rausch, Philipp, et al. (2019), 'Comparative analysis of amplicon and metagenomic sequencing methods reveals key features in the evolution of animal metaorganisms', *Microbiome*, 7 (1),
- Rehman, A, et al. (2016), 'Geographical patterns of the standing and active human gut microbiome in health and IBD.', *Gut*, 65 (2), 238-48.
- Reichardt, Nicole, et al. (2018), 'Specific substrate-driven changes in human faecal microbiota composition contrast with functional redundancy in short-chain fatty acid production', *The ISME Journal*, 12 (2), 610-22.
- Ricklin, D, et al. (2016), 'Complement component C3 - The "Swiss Army Knife" of innate immunity and host defense.', *Immunol. Rev.*, 274 (1), 33-58.
- Rieseberg, Loren H, Margaret A Archer, and Robert K Wayne (1999), 'Transgressive segregation, adaptation and speciation', *Heredity*, 83 (4), 363-72.
- Rolig, AS, et al. (2015), 'Individual Members of the Microbiota Disproportionately Modulate Host Innate Immune Responses.', *Cell Host Microbe*, 18 (5), 613-20.
- Rosshart, Stephan P., et al. (2017), 'Wild Mouse Gut Microbiota Promotes Host Fitness and Improves Disease Resistance', *Cell*, 171 (5), 1015-1028.e13.
- Roth, TL, et al. (2019), 'Reduced Gut Microbiome Diversity and Metabolome Differences in Rhinoceros Species at Risk for Iron Overload Disorder.', *Front Microbiol.*, 10 2291.
- Rowland, Ian, et al. (2018), 'Gut microbiota functions: metabolism of nutrients and other food components', *European Journal of Nutrition*
Eur J Nutr, 57 (1), 1-24.
- Rühlemann, Malte Christoph, et al. (2021), 'Genome-wide association study in 8,956 German individuals identifies influence of ABO histo-blood groups on gut microbiome', *Nat. Genet.*, 1-9.
- Saito, Yumiko, et al. (1999), 'Molecular characterization of the melanin-concentrating-hormone receptor', *Nature*, 400 (6741), 265-69.
- Sarkar, Amar, et al. (2020), 'The role of the microbiome in the neurobiology of social behaviour', *Biol. Rev.*, 95 (5), 1131-66.
- Sethi, JK and AJ Vidal-Puig (2008), 'Wnt signalling at the crossroads of nutritional regulation.', *Biochem. J.*, 416 (2), e11-3.
- Shannon, Paul, et al. (2003), 'Cytoscape: a software environment for integrated models of biomolecular interaction networks', *Genome Research*
Genome Res, 13 (11), 2498-504.
- Shi, L and BP Tu (2015), 'Acetyl-CoA and the regulation of metabolism: mechanisms and consequences.', *Curr. Opin. Cell Biol.*, 33 125-31.
- Singh, Parul, et al. (2020), 'The potential role of vitamin D supplementation as a gut microbiota modifier in healthy individuals', *Scientific Reports*, 10 (1), 21641.
- Škrabar, N, et al. (2018), 'Using the *Mus musculus* hybrid zone to assess covariation and genetic architecture of limb bone lengths.', *Mol Ecol Resour.*, 18 (4), 908-21.
- Smith, Ashley E., et al. (2019), 'Binge-Type Eating in Rats is Facilitated by Neuromedin U Receptor 2 in the Nucleus Accumbens and Ventral Tegmental Area', *Nutrients*, 11 (2), 327.
- Snijders, Antoine M., et al. (2016), 'Influence of early life exposure, host genetics and diet on the mouse gut microbiome and metabolome', *Nature Microbiology*, 2 16221.
- Spor, Aymé, Omry Koren, and Ruth Ley (2011), 'Unravelling the effects of the environment and host genotype on the gut microbiome', *Nature Reviews Microbiology*, 9 (4), 279-90.
- Sriram, K and PA Insel (2018), 'G Protein-Coupled Receptors as Targets for Approved Drugs: How Many Targets and How Many Drugs', *Mol. Pharmacol.*, 93 (4), 251-58.
- Steffen Durinck, Paul T. Spellman, Ewan Birney and Wolfgang Huber (2009), 'Mapping identifiers for the integration of genomic datasets with the R/Bioconductor package biomaRt.', *Nature Protocols*, 4 1184-91.
- Suzuki, TA (2017), 'Links between Natural Variation in the Microbiome and Host Fitness in Wild Mammals.', *Integr Comp Biol*, 57 (4), 756-69.
- Suzuki, TA, et al. (2020), 'The gut microbiota and Bergmann's rule in wild house mice.', *Mol Ecol*, 29 (12), 2300-11.

- Suzuki, Taichi A and Ruth E Ley (2020), 'The role of the microbiota in human genetic adaptation', *Science*, 370 (6521),
- Suzuki, Taichi A., et al. (2019), 'Host genetic determinants of the gut microbiota of wild mice', *Molecular Ecology*, 28 (13), 3197-207.
- Szklarczyk, Damian, et al. (2019), 'STRING v11: protein-protein association networks with increased coverage, supporting functional discovery in genome-wide experimental datasets', *Nucleic Acids Research*
- Nucleic Acids Res*, 47 (D1), D607-13.
- Tanahashi, Yasuyuki, et al. (2009), 'Multiple muscarinic pathways mediate the suppression of voltage-gated Ca²⁺ channels in mouse intestinal smooth muscle cells', *Br. J. Pharmacol.*, 158 (8), 1874-83.
- Taras, David, et al. (2002), 'Reclassification of *Eubacterium formicigenerans* Holdeman and Moore 1974 as *Dorea formicigenerans* gen. nov., comb. nov., and description of *Dorea longicatena* sp. nov., isolated from human faeces.', *International Journal of Systematic and Evolutionary Microbiology*, 52 (2), 423-28.
- Thaiss, Christoph A., et al. (2014), 'Transkingdom control of microbiota diurnal oscillations promotes metabolic homeostasis', *Cell*, 159 (3), 514-29.
- Thaiss, Christoph A., Maayan Levy, and Eran Elinav (2015a), 'Chronobiomics: The Biological Clock as a New Principle in Host-Microbial Interactions', *PLoS Pathog.*, 11 (10), e1005113.
- Thaiss, Christoph A., et al. (2015b), 'A day in the life of the meta-organism: diurnal rhythms of the intestinal microbiome and its host', *Gut Microbes*, 6 (2), 137-42.
- Thaiss, Christoph A., et al. (2016), 'Microbiota Diurnal Rhythmicity Programs Host Transcriptome Oscillations', *Cell*, 167 (6), 1495-1510.e12.
- Tian, Liang, et al. (2020), 'Deciphering functional redundancy in the human microbiome', *Nature Comm.*, 11 (1),
- Toderici, M, et al. (2016), 'Identification of Regulatory Mutations in SERPINC1 Affecting Vitamin D Response Elements Associated with Antithrombin Deficiency.', *PLoS One*, 11 (3), e0152159.
- Townsend, KL, et al. (2012), 'Bone morphogenetic protein 7 (BMP7) reverses obesity and regulates appetite through a central mTOR pathway.', *FASEB J.*, 26 (5), 2187-96.
- Turnbaugh, Peter J., et al. (2009), 'A core gut microbiome in obese and lean twins', *Nature*, 457 (7228), 480-84.
- Turnbaugh, PJ, et al. (2008), 'Diet-induced obesity is linked to marked but reversible alterations in the mouse distal gut microbiome.', *Cell Host Microbe*, 3 (4), 213-23.
- Turner, Leslie M., Denise J. Schwahn, and Bettina Harr (2012), 'Reduced Male Fertility Is Common but Highly Variable in Form and Severity in a Natural House Mouse Hybrid Zone', *Evolution*, 66 (2), 443-58.
- Turner, Leslie M. and Bettina Harr (2014), 'Genome-wide mapping in a house mouse hybrid zone reveals hybrid sterility loci and Dobzhansky-Muller interactions', *eLife*, 3 e02504.
- Turpin, W., et al. (2016), 'Association of host genome with intestinal microbial composition in a large healthy cohort', *Nat. Genet.*, 48 (11), 1413-17.
- Valerie, Obenchain, et al. (2014), 'VariantAnnotation: a Bioconductor package for exploration and annotation of genetic variants', *Bioinformatics*, 30 (14), 2076-78.
- Velloso, Licio A., Franco Folli, and Mario J. Saad (2015), 'TLR4 at the Crossroads of Nutrients, Gut Microbiota, and Metabolic Inflammation', *Endocrine Reviews*
- Endocr Rev*, 36 (3), 245-71.
- Wang, Jun, et al. (2015), 'Analysis of intestinal microbiota in hybrid house mice reveals evolutionary divergence in a vertebrate hologenome', *Nature Communications*
- Nat Commun*, 6
- Wang, Jun, et al. (2016), 'Genome-wide association analysis identifies variation in vitamin D receptor and other host factors influencing the gut microbiota', *Nat. Genet.*, 48 (11), 1396-406.
- Weldon, L, et al. (2015), 'The Gut Microbiota of Wild Mice.', *PLoS One*, 10 (8), e0134643.
- Wu, Guangyan, et al. (2018), 'Light exposure influences the diurnal oscillation of gut microbiota in mice', *Biochemical and Biophysical Research Communications*
- Biochem Biophys Res Commun*, 501 (1), 16-23.
- Yang, Q, et al. (2020), 'Role of Dietary Nutrients in the Modulation of Gut Microbiota: A Narrative Review.', *Nutrients*, 12 (2), E381.
- Yasuda, K, et al. (2021), 'Elucidation of metabolic pathways of 25-hydroxyvitamin D₃ mediated by CYP24A1 and CYP3A using Cyp24a1 knockout rats generated by CRISPR/Cas9 system.', *J. Biol. Chem.*, 296 100668.
- Yatsunenko, Tanya, et al. (2012), 'Human gut microbiome viewed across age and geography', *Nature*, 486 (7402), 222-27.

Yi, Z and GA Bishop (2015), 'Regulatory role of CD40 in obesity-induced insulin resistance.', *Adipocyte*, 4 (1), 65-69.

Yu, Guangchuang, et al. (2012), 'clusterProfiler: an R package for comparing biological themes among gene clusters', *OmicS: a journal of integrative biology*, 16 (5), 284-87.

Zhou, Xiang and Matthew Stephens (2012), 'Genome-wide efficient mixed-model analysis for association studies', *Nat. Genet.*, 44 (7), 821-24.

Ziyatdinov, Andrey, et al. (2018), 'lme4qtl: linear mixed models with flexible covariance structure for genetic studies of related individuals', *BMC Bioinformatics*, 19 (1), 1-5.